INDEX OF ABUNDANCE OF JUVENILE SKIPJACK TUNA IN THE INDIAN OCEAN DERIVED FROM ECHO-SOUNDER BUOY DATA (2012-2024).

Jon Uranga[1], Guillermo Boyra[1], Jaime Perez[1], Maitane Grande[1], Gorka Merino[1], Agurtzane Urtizberea[1], Haritz Harrizabalaga[1]

SUMMARY

Collaboration between Spanish vessel-owner associations and buoy providers has enabled the retrieval of data from satellite-linked GPS tracking echosounder buoys deployed by tropical tuna purse seiners operating in the Indian Ocean since 2012. These buoys transmit real-time information on Fish Aggregating Device (FAD) positions and acoustic estimates of fish biomass beneath them.Echosounder buoys provide a valuable source of fishery-independent data to monitor tuna aggregations. However, the acoustic signal represents an integrated biomass that does not distinguish species or size composition. To overcome this limitation, buoy data must be combined with fishery information, including species composition and size structure, to derive species-specific indicators.This study presents an updated abundance index of juvenile skipjack tuna in the Indian Ocean based on echosounder buoy data for the period 2012–2024.

[1] AZTI, Marine Research, Basque Research and Technology Alliance (BRTA). Txatxarramendi ugartea z/g, 48395. Sukarrieta - Bizkaia, Spain

1. Introduction

Stock assessments of tropical tuna have traditionally relied on abundance indicators derived from commercial catch and effort information reported in logbooks or by onboard observers (Maunder & Punt, 2004). For highly migratory species such as tunas, where fishery-independent surveys are generally not feasible, most indices used in stock assessment are based on catch-per-unit-effort (CPUE), which relates catch or biomass to a measure of fishing effort (Quinn & Deriso, 1999).

CPUE-based indices assume a proportional relationship between abundance and catchability (q). However, this relationship may be affected by changes in fishing efficiency, spatial and temporal shifts in fleet or stock distribution, and environmental variability (Maunder & Punt, 2004; Maunder et al., 2006). To account for these sources of variation, standardization approaches are commonly applied to better isolate signals associated with population dynamics.

The progressive adoption of new fishing technologies, particularly the widespread use of Fish Aggregating Devices (FADs) in tropical tuna purse seine fisheries, has substantially increased fishing efficiency (Gaertner, Ariz, et al., 2016; Lopez et al., 2014; Torres-Irineo et al., 2014). This evolution has introduced additional challenges for CPUE standardization, including the need to incorporate fine-scale covariates that reflect technological developments and effort creep. In addition, the lack of a robust proxy for purse-seine effort in FAD fisheries further complicates the derivation of reliable indices (Gaertner, Clermidy, et al., 2016; Katara, 2018; Wain, 2021). Consequently, the use of CPUE from FAD-associated fisheries in stock assessments has been subject to limitations in several RFMO processes. Continued collaboration between science and industry is therefore essential to improve data availability and methodological approaches for integrating technological effects into CPUE standardization (Wain, 2021).

In this context, satellite-linked echosounder buoys deployed on FADs provide an alternative data source to monitor fish aggregations and derive fishery-independent indices (Scott, 2014). These buoys deliver regular information on position and acoustic estimates of biomass beneath the FAD, enabling systematic and non-invasive observation of aggregation dynamics. However, current buoy systems provide integrated acoustic signals without information on species composition or size structure. As a result, the combination of echosounder data with auxiliary fishery information is required to derive species-specific indicators, such as for skipjack tuna.

The availability of these data has been made possible through collaboration with the Spanish purse-seine sector, including vessel-owner associations (ANABAC and OPAGAC) and buoy providers (Marine Instruments, Satlink and Zunibal). This partnership has enabled access to historical records from echosounder buoys used by the Spanish tropical tuna fleet operating in the Indian Ocean over the period 2012–2024. In parallel, methodological developments have been undertaken to extract robust scientific information from these data (Orue et al., 2019). These datasets have supported studies on tuna behaviour and ecology around FADs, and have contributed to the development of buoy-derived abundance indices (Baidai, 2020; Capello et al., 2016; Lopez et al., 2014; Moreno, 2016; Orue et al., 2019; Santiago et al., 2019).

Comparable indices were previously developed for the Atlantic Ocean (Santiago et al., 2019), covering the three main tropical tuna species (skipjack, yellowfin, and bigeye) (Santiago et al., 2021a, 2021b). In the Pacific Ocean, buoy-based abundance indices have also been explored, including their incorporation into interim skipjack assessments conducted by IATTC (Uranga, 2021, 2023, 2024). These efforts demonstrate the potential of echosounder buoy data to complement traditional indices and contribute to future assessments across ocean basins.

The present study provides an updated abundance index for skipjack tuna in the Indian Ocean, derived from echosounder buoy data for the period 2012–2024.

2. Material and methods

2.1 The acoustic data

The primary data used in this analysis was collected by satellite-linked echo-sounder buoys attached to Fish Aggregating Devices (FADs) used in the Indian Ocean tropical tuna purse-seine fishery. Specifically, only data provided by the buoy manufacturer Satlink was used in this analysis. Technical specifications for each buoy model

are presented in Table 1. The buoys record information from a depth of 3 to 115 meters, divided into ten uniform vertical layers, each with a resolution of 11.2 meters. Note that the first 3 meters are considered the blind zone and do not provide usable data. Five different buoy models (DS+, DSL+, ISD+, ISL+, and SLX+) were used during the analyzed period (January 2012 to December 2024) (Table 1).

The database for this analysis included a total of 24 million acoustic records from 109242 individual buoys. Figure 1 shows how the fleet has been using various types of models throughout the study period. Additionally, acoustic records from areas with a low number of observations (less than 100 records in 5^{o}x5^{o} statistical rectangles) were discarded from the analysis.

ANABAC and OPAGAC have provided acoustic information and species-specific catch percentages at 1x1 degree resolution from their echosounder buoys. From each single data record, transmitted via satellite, the following information was extracted: “Name”, unique identification number of the buoy, given by the model code (DS+, DSL, ISL, ISD, SLX) followed by 5-6 digits; “OwnerName“, name of the buoy owner assigned to a unique purse seine vessel; “MD“, message descriptor (160, 161 and 162 for position data, without echosounder data, and 163, 168, 169 and 174 for echosounder data); “StoredTime“, date (dd/mm/yyyy) and hour (HH:MM) of the position and the echosounder records; “Latitude, Longitude“, record-associated GPS latitude and longitude information (in decimals); “Bat“, battery charge level of the buoy, as a percentage (not provided, except for the D+ and DS+ models, in voltage); “Speed“, estimated speed of the buoy in knots; “Layer1-Layer10“, estimated tons of tuna by layer (values are estimated by a manufacturer´s method which converts raw acoustic backscatter into biomass in tons, using a depth layer echo-integration procedure based exclusively on an algorithm using the target strength (TS) and weight of skipjack tuna); “Sum“, sum of the biomass estimated for all layers; “Max“, maximum biomass estimated at any layer; and “Mag1, Mag3, Mag5 and Mag7“, magnitudes corresponding to the counts of detected targets according to the TS of the detection peak.

To eliminate artifacts, we applied a set of five filters to the original data. These filters were designed to remove: 1) isolated, duplicated, and ubiquitous rows, which are often caused by satellite communication issues; 2) buoys located within 1 km of land or in continental shelf areas (i.e., those with bottom depths shallower than 200 m), which were identified and removed using shoreline data from the GSHHG database (Wessel, 1996) and a worldwide global bathymetry information (Amante & Eakins, 2009); and 3) “on-board” or “at sea” positions, which were identified using a Random Forest algorithm (Orue et al., 2019; Santiago et al., 2020). These cases typically occur when a buoy is activated onboard a vessel prior to deployment or post-retrieval. Acoustic records equal or less than 0.01 tonnes were considered zeros. This is a conservative preliminary value since further validation is needed.

In addition to the data cleaning filters mentioned earlier, the following selection criteria (Santiago et al. 2020) were used to create the final dataset for the standardization analysis. Firstly, shallower layers (<25m) were excluded because they are considered to potentially reflect non-tuna species (e.g., Orue et al., 2019). Secondly, only data recorded around sunrise, between 4 a.m. and 8 a.m. in local time, were considered for the analysis as they are believed to better capture the biomass under the FADs. Finally, acoustic data belonging to “virgin segments” were selected to use the segment of a buoy trajectory whose associated FAD likely represents a new deployment that has been potentially colonized by tuna and not fished yet. To calculate virgin segments, single buoy information was divided into smaller segments where the difference between two consecutive observations of the same buoy was larger than 30 days. Although this may represent buoys that have been re-deployed at a reasonable rate, it seems unlikely. However, segments with less than 30 observations and those having a time difference between any of the consecutive observations longer than 4 days during the first 35 days were removed. Finally, from the remaining data, information corresponding to 20-35 days at sea was used as this is the time period for which FADs seem to be colonized (Orue et al. 2019). Figure 2 shows a diagram with an example of “virgin” segments used to calculate the BAI index.

2.2 From acoustic data to a species-specific abundance indicator

To calculate the biomass aggregated under a FAD from the acoustic signal, Satlink uses the density of one species, skipjack, to provide the biomass in tons, biomass data from Satlink was converted to decibels reversing their formula for the biomass computation. Then we recomputed biomass using standard abundance estimations equations (Simmonds & MacLennan, 2005):

$$Biomass_i = \frac{s_V \cdot Vol \cdot p_i}{\sum_i \sigma_i \cdot p_i}$$

where *Sv* is the volume backscattering strength, *Vol* is the sampled volume and p_i and σ_i are the proportion and linearized target strength of each species *i* respectively. Species proportions in weight were extracted from the logbooks of the fleet associated to OPAGAC (19 vessels) for each 1ºx1º and month stratum, as explained below. Mean fish lengths (L_i) used for skipjack (SKJ), bigeye (BET) and yellowfin (YFT) were obtained from ICCAT T2CS - catch-at-size, and weights were obtained using weight-length relationships (ICCAT conversion factors). Then, the following TS-length relationships were used to obtain linearized target strength per kilogram:

$$\sigma_i = \frac{10^{(TS)/10}}{w_i}$$

where w_i is the mean weight of each species and *TS* is the backscattering cross-section of each species individual fish. It is assumed that the linear value of TS, is proportional to the square of fish length (Simmons and MacLennan 2005).

$$TS_i = 20\log(L_i) + b_{20,i}$$

Given that each brand uses different operating frequencies, we used different b20 values for each species. For Satlink, the b20 values were obtained from (Boyra et al., 2018) for SKJ, from (Sobradillo et al., 2024) for YFT and from (Boyra et al., 2019) for BET.

Since acoustic records do not always contain species composition at matching time–area strata, we implemented a five-step hierarchical assignment based on progressively coarser spatio-temporal resolutions to populate species-specific acoustic signals (yft, bet, skj) and derive species composition percentages. The information was sourced from fishery-dependent data provided by the tuna purse-seine fleet, specifically from the ANABAC and OPAGAC associations, which represent a substantial fraction of the fleet.

The hierarchical strata were defined sequentially (from highest to lowest resolution) to assign species composition information to the acoustic data. Observations were matched at the highest resolution level first; if data were insufficient, the criteria were progressively relaxed until a suitable species composition profile was available. The hierarchical structure was defined as follows: strata level 1 consisted of a 1x1 degree spatial grid by month and year; strata level 2 expanded to a 5x5 degree spatial grid by month and year; strata level 3 utilized the official IOTC management regions by month and year; strata level 4 relaxed the temporal resolution to a 5x5 degree spatial grid by quarter and year; and finally, strata level 5 applied the IOTC management regions by quarter and year.

IOTC regions were defined according to latitude–longitude thresholds as large spatial aggregates: Region 1 (lat > 25°N and lon < 35°W), Region 2 (lat > 10°N and lon ≥ 35°W), Region 3 (lat < 25°N and lon < 35°W), Region 4 (lat < 10°N and lon ≥ 35°W), and Region 5 (lat ≤ 10°S).

The number of observations assigned at each spatio-temporal resolution level is shown in Figure 3. The highest-resolution assignments (strata 1 and 2) are predominantly concentrated in the western and central Indian Ocean, particularly along the East African coast (Somalia–Mozambique channel) and extending eastward between ~5°N and 15°S up to ~65–70°E, reflecting the main operational areas of the purse-seine fleet.

The results presented in this document correspond to the fraction of the acoustic signal estimated to be informative for the biomass of skipjack tuna.

2.3 The BAI index: Buoy-derived Abundance Index

The estimator of abundance BAI was defined as the 0.9 quantile of the integrated acoustic energy observations in each of the "virgin" sequences. A high quantile was chosen because the large values are considered to be likely produced by tuna (in opposition to plankton or bycatch species). This assumption is followed by all the buoy brands in the market, which use the maximum value as the summary of each time interval. In our case we selected a high quantile instead of the maximum to try to provide a more robust estimator by avoiding eventual outlier values. We did this to avoid considering the expected lowest values that might appear after eventual

hauls occurring along the sequence. The total number of "virgin" sequences retained after filtering, ensuring that all tracks corresponded to new deployments and therefore defining the number of observations used in the model, was 66,699. Of these, 99.7% were positive observations, with estimated biomass values equal to or greater than 0.01 tonnes.

2.4 The model

The covariates used in the standardization process and fitted as categorical variables were year-quarter, 1x1^{o} area, and buoy model.

The explanatory variables included temporal (*yyqq*), spatial (*area*), and buoy configuration (*model*) factors, together with a set of environmental covariates describing oceanographic conditions. Temporal variability was represented at a quarterly resolution, while spatial structure was accounted for through predefined analysis areas. Differences among buoy models were included to account for potential variability in acoustic measurements. Environmental variables comprised chlorophyll concentration (*chl*) and its gradient (*chlfront*), mixed layer depth (*mld*), subsurface temperature (*Thetao*), sea surface temperature (*sst*), current intensity (*current*), and mean wave conditions (*wav_mean*). Interaction terms between temporal and spatial factors (*yyqq:area*) and between temporal and buoy model factors (*yyqq:model*) were also incorporated to capture spatio-temporal variability and potential differences in trends among buoy types.

The model assumes that the signal from the echosounder is proportional to the abundance of fish under the FAD, which is similar to the fundamental relationship between CPUE and abundance used in quantitative fisheries analysis:

$$BAI_t = \varphi \, . B_t$$

where BAIt is the Buoy-derived Abundance Index and Bt is the abundance in time t (Santiago et al., 2016).

Resolving the relationship between acoustic indicators and fishing performance is not straightforward. It is assumed that acoustic echo integration is a linear process, i.e., proportional to the number of targets (Simmons & MacLennan, 2005) and has been experimentally proven to be correct with some limitations (Foote, 1983; Røttingen, 1976). Therefore, acoustic data (echo integration) is commonly taken as an estimator of abundance and is thoroughly applied to provide acoustic estimation of abundance of many pelagic species (Hampton, 1996; Masse et al., 2018).

As with the catchability, the coefficient of proportionality ϕ is not constant for many reasons. In order to ensure that ϕ can be assumed to be constant (i.e. to control the effects other than those caused by changes in the abundance of the population) a standardization analysis should be performed aiming to remove factors other than changes in abundance of the population. This can be performed standardizing nominal measurements of the echosounders using a Generalized Linear Mixed Modelling (GLMM) approach.

Considering the low proportion of zero values (0.3%) the delta lognormal approach (Lo et al., 1992) was not considered. GLMM (log-normal error structured model) was applied to standardize the acoustic observations. A stepwise procedure was used to fit the model with all the explanatory variables and interactions to determine those that significantly contributed to explaining the variability of the data. For this, deviance analysis tables were created for the positive acoustic records. Final selection of explanatory variables was conducted using a) the relative percent increase in deviance explained when the variable was included in the model (normally variables that explained more than 5% were selected), and b) The Chi-square (χ2) significance test. Those variables that explained less than 5% of the variability in the data were not considered for the final model.

Interactions between the temporal component (year-quarter) with the rest of the variables were also evaluated. If an interaction was statically significant, it was then considered as a random interaction(s) within the final model (Maunder & Punt, 2004).

The selection of the final mixed model was based on the Akaike's Information Criterion (AIC), the Bayesian Information Criterion (BIC), and a Chi-square ($\chi 2$) test of the difference between the log-likelihood statistic of different model formulations. The year-quarter effect least square means (LSmeans) were bias corrected for the logarithm transformation algorithms using Lo et al (1992). All analyses were done using the lme4 package for R (Bates et al., 2014).

Based on the Analysis of Deviance of table 2 the most significant explanatory factors were incorporated in the following lognormal model, where the proportion of deviance explained by the model was 41.39% and interactions were considered as random effects:

$$\log(index) \sim yyqq + area + model + (yyqq : area)$$

3. Results

A total of 24,009,385 records from more than 109,242 individual buoys were compiled for the period January 2012 to December 2024. After applying the filtering criteria and selecting "virgin" segments, the dataset was reduced to 66,699 observations used in the GLM analysis. Each observation was calculated as the 90% percentile of a "virgin" segment of buoy trajectories. A virgin segment was defined as the segment of a buoy trajectory from 20-35 days at sea, so that the associated FAD likely represents a new deployment which has been potentially colonized by tuna and not already fished.

In this analysis we have obtained from the acoustic signal of the echosounder buoys associated to FADs the biomass of skipjack tuna aggregated under a FAD.

The spatial distribution of the dominant species composition assignment classes is shown in Figure 3. The results reveal a marked spatial structure across the Indian Ocean, with distinct regions characterized by different dominant assignment levels. Lower resolution classes are predominantly observed in offshore and central areas, whereas higher resolution classes are more frequently associated with regions of higher data density, particularly along coastal zones.Transitional areas between classes are also evident, reflecting gradual changes in assignment resolution across space. These patterns are consistent with the spatial distribution of observations and highlight the influence of data availability on the assignment procedure. Overall, the results underline the heterogeneous nature of the dataset and the importance of accounting for spatial variability in the characterization of species composition.

Figure 4 shows the histograms of the BAI and log transformed BAI nominal values. Log transformation makes the data to follow a normal distribution, as shown in the left panel.

The spatial distribution of "virgin" sequences retained for the GLM analysis is shown in Figure 5. The results indicate a heterogeneous spatial distribution across the study area, with higher concentrations of observations in the western equatorial and central regions of the Indian Ocean, particularly off East Africa and around the Mozambique Channel. In contrast, lower densities are observed in peripheral offshore areas and southern latitudes. This spatial pattern reflects the distribution of fishing activity and buoy deployments, as well as the filtering applied to retain only suitable segments for the analysis.

The temporal evolution of the number of observations, aggregated by quarter and 5° × 5° grid cells, is presented in Figure 6. The results show a general increase in data availability over time although the temporal trends vary considerably across areas. Some grid cells display relatively stable time series, while others exhibit marked fluctuations or more recent increases in the number of observations. These differences highlight the uneven spatio-temporal coverage of the dataset and underline the importance of accounting for both spatial and temporal variability in the modelling framework.

Independent variables tested in the GLM included year-quarter (yyqq), 5ºx5º area (area), buoy model (model), and environmental drivers (chl, chlfront, mld, Thetao, sst, current, and wav_mean). The dependent variable was the log-transformed Buoy-derived Abundance Index (log BAI) based on the 0.9 quantile of the acoustic energy in the "virgin" sequence. As shown in Table 2, the model explained 25.95% of the total deviance. The primary explanatory factors were area (8.33%), the yyqq:area interaction (8.30%), and yyqq (6.61%), all highly significant

(P < 0.001$). Among environmental variables, wav_mean (0.71%) and mld (0.25%) had the largest effects, while chlfront was non-significant.

No systematic residual patterns were observed (Figure 7). Residual diagnostics for the positive observations model (log-biomass) showed strong compliance with standard GLM assumptions (Figure 7). The residuals vs. fitted values plot (Figure 7a) indicated homoscedasticity, with the GAM smoothing line remaining flat and centered at zero, showing no systematic bias. The Normal Q-Q plot (Figure 7b) and the residual histogram (Figure 7c) confirmed the normality of the error distribution, displaying excellent alignment with the theoretical Gaussian curve except for minor deviations in the extreme lower tail. The log-transformation successfully normalized the abundance index.

The Buoy-derived Abundance Index (BAI) time series for the 2012–2024 period revealed distinct, highly dynamic trends among the three tropical tuna species (Figure 8).

The core output of this standardization is represented by the main Skipjack tuna (SKJ) biomass index (Figure 8a). This primary result filters operational and environmental noise while tracking the nominal fluctuations with high precision, as demonstrated by the narrow 95% confidence intervals.

Notably, the SKJ standardized index exhibits a clear, overall positive trend throughout the study period, characterized by steadily increasing abundance peaks and rising historical baselines, particularly from 2018 onwards.

While the SKJ biomass remains the central focus, the quarterly species composition proportion (Figure 8b) and the multi-species macro-trends (Figure 8c) have been explicitly included to provide the complete picture. By displaying each index on its own scale, we avoid masking the critical differences in their true orders of magnitude. This comprehensive view uncouples the absolute dominance of SKJ in terms of relative biomass, while showing that Yellowfin (YFT) and Bigeye (BET) tunas maintain much lower, stable multi-annual trajectories over time.

Acknowledgements

This study was funded by the Basque Government (Department of Economic Development, Sustainability and Environment). The authors acknowledge the support of the Spanish vessel owner associations ANABAC and OPAGAC, as well as all companies that provided acoustic data from their echosounder buoys. We also thank the buoy providers Marine Instruments, Satlink and Zunibal for facilitating access to these data.

Tables and figures

Model	Typical setup						Mean observed values over analysis data	
	Beam angle	Sounder frequency	Power	Frequency of acoustic sampling (ping rate)	Daily acoustic data recorded	Frequency of transmission	Number of buoys	Sampling frequency
DS+	32º	190.5 kHz	100 W	3	3	24h	1428	1.36
DSL+	32º	190.5 kHz	100 W	3	3	24h	12462	2.82
ISL+	32º	190.5 kHz	100 W	15 min	variable (reset at dusk)	24h	23	1.67
ISD+	32º	200/38 kHz (38 kHz not provided)	100 W	15 min	variable (reset at dusk)	24h	6214	1.21
SLX+	32º	200	100 W	5 min	variable (Sunrise or Alarms based)	24h	785	1.98

Table 1. Technical specifications of different buoy models and observed values over analysis data.

Variable	Deviance	Resid_df	Resid_dev	F	Pr(>f)	Dev_exp
Yyqq	8990	66846	127097	114	0	6,61
Area	11342	66810	115755	203	0	8,33
Model	856	66807	114900	184	0	0,63
Chl	12	66806	114888	8	0	0,01
Chlfront	0	66805	114888	0	1	0
Mld	338	66804	114550	218	0	0,25
Thetao	109	66803	114440	71	0	0,08
Sst	11	66802	114429	7	0	0,01
Current	99	66801	114330	64	0	0,07
Wav_mean	961	66800	113369	620	0	0,71
Yyqq:area	11293	65200	102076	5	0	8,3
Yyqq:model	1159	65126	100917	10	0	0,85

Table 2. Deviance table for the lognormal GLM fitted to the 2012–2024 period. Columns show: predictor; Deviance, reduction in deviance explained by each predictor; Resid_df, residual degrees of freedom after adding the predictor; Resid_dev, residual deviance; F, F-statistic testing the significance of each predictor; Pr(>F), associated p-value; and Dev_exp, percentage of total deviance explained by each predictor.

Quarter	Index_nominal	Bai_index	Bai_se	Bai_cv
12Q1	2,23	1,941	0,52	0,268
12Q2	1,572	1,371	0,328	0,239
12Q3	0,728	0,769	0,144	0,187
12Q4	1,646	1,473	0,275	0,187
13Q1	1,56	1,393	0,25	0,18
13Q2	1,611	1,253	0,21	0,168
13Q3	0,765	0,826	0,118	0,142
13Q4	1,708	1,381	0,211	0,153
14Q1	2,628	1,949	0,305	0,156
14Q2	1,912	1,554	0,234	0,15
14Q3	1,171	1,157	0,153	0,133
14Q4	1,604	1,313	0,184	0,14
15Q1	1,943	1,884	0,24	0,127
15Q2	1,235	1,13	0,157	0,139
15Q3	1,43	1,198	0,148	0,124
15Q4	1,095	1,046	0,132	0,126
16Q1	1,436	1,444	0,152	0,105
16Q2	1,237	1,213	0,155	0,127
16Q3	1,357	1,248	0,145	0,116
16Q4	1,363	1,205	0,141	0,117
17Q1	2,048	1,828	0,219	0,12
17Q2	1,921	1,636	0,212	0,129
17Q3	2,067	1,999	0,229	0,115
17Q4	1,811	1,847	0,263	0,143
18Q1	2,119	2,074	0,274	0,132
18Q2	1,998	1,669	0,245	0,147
18Q3	2,939	3,069	0,394	0,128
18Q4	2,491	2,166	0,323	0,149
19Q1	2,613	2,597	0,372	0,143
19Q2	1,828	1,553	0,241	0,155
19Q3	2,143	1,943	0,283	0,145
19Q4	3,13	2,971	0,464	0,156
20Q1	2,806	2,784	0,392	0,141
20Q2	1,939	1,763	0,237	0,134
20Q3	2,192	2,312	0,276	0,119
20Q4	2,095	1,792	0,26	0,145
21Q1	2,703	2,502	0,324	0,129
21Q2	2,823	2,576	0,346	0,134
21Q3	3,543	3,349	0,442	0,132
21Q4	2,512	2,394	0,324	0,135
22Q1	3,156	3,033	0,364	0,12
22Q2	2,287	2,259	0,273	0,121
22Q3	3,068	2,851	0,32	0,112
22Q4	2,582	2,33	0,284	0,122
23Q1	3,243	3,027	0,406	0,134

23Q2	2,163	2,023	0,28	0,139
23Q3	3,067	2,85	0,384	0,135
23Q4	3,162	2,822	0,437	0,155
24Q1	4,392	4,009	0,524	0,131
24Q2	3,93	3,343	0,478	0,143
24Q3	3,867	3,907	0,508	0,13
24Q4	2,71	2,454	0,397	0,162

Table 3. Nominal and standardized Buoy-derived Abundance Index for the period 2012-2024. Standard errors and coefficient of variations of the standardized series are also included.

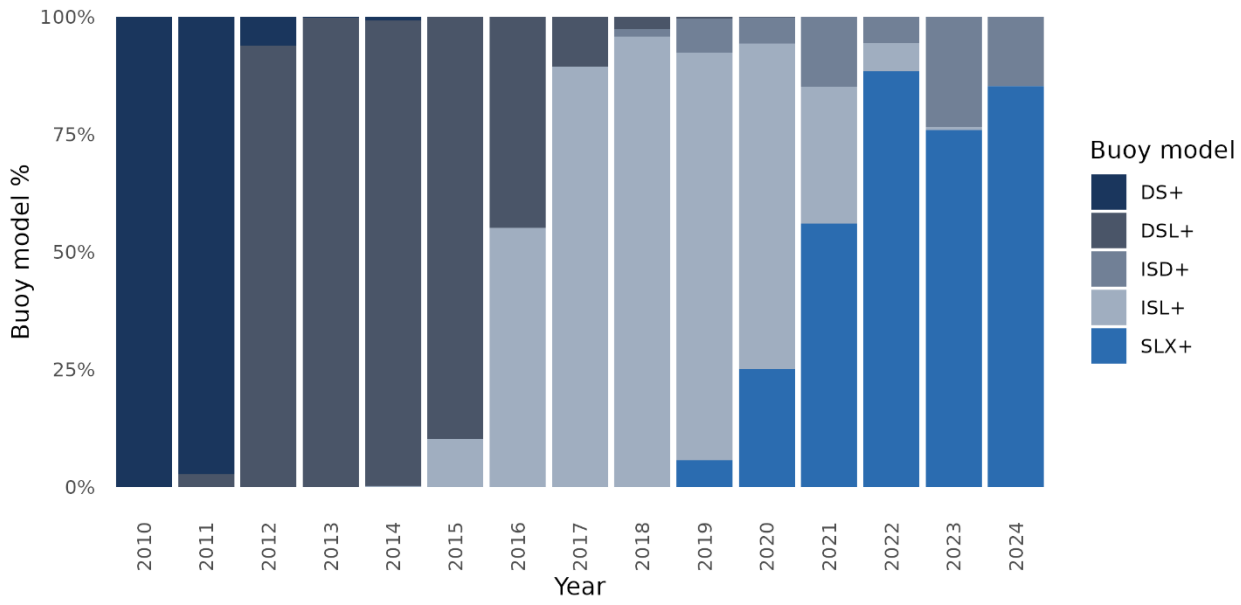

Figure 1. Evolution over time of the buoys utilized by the purse seine fleet in the Indian Ocean during the study period (2012-2024).

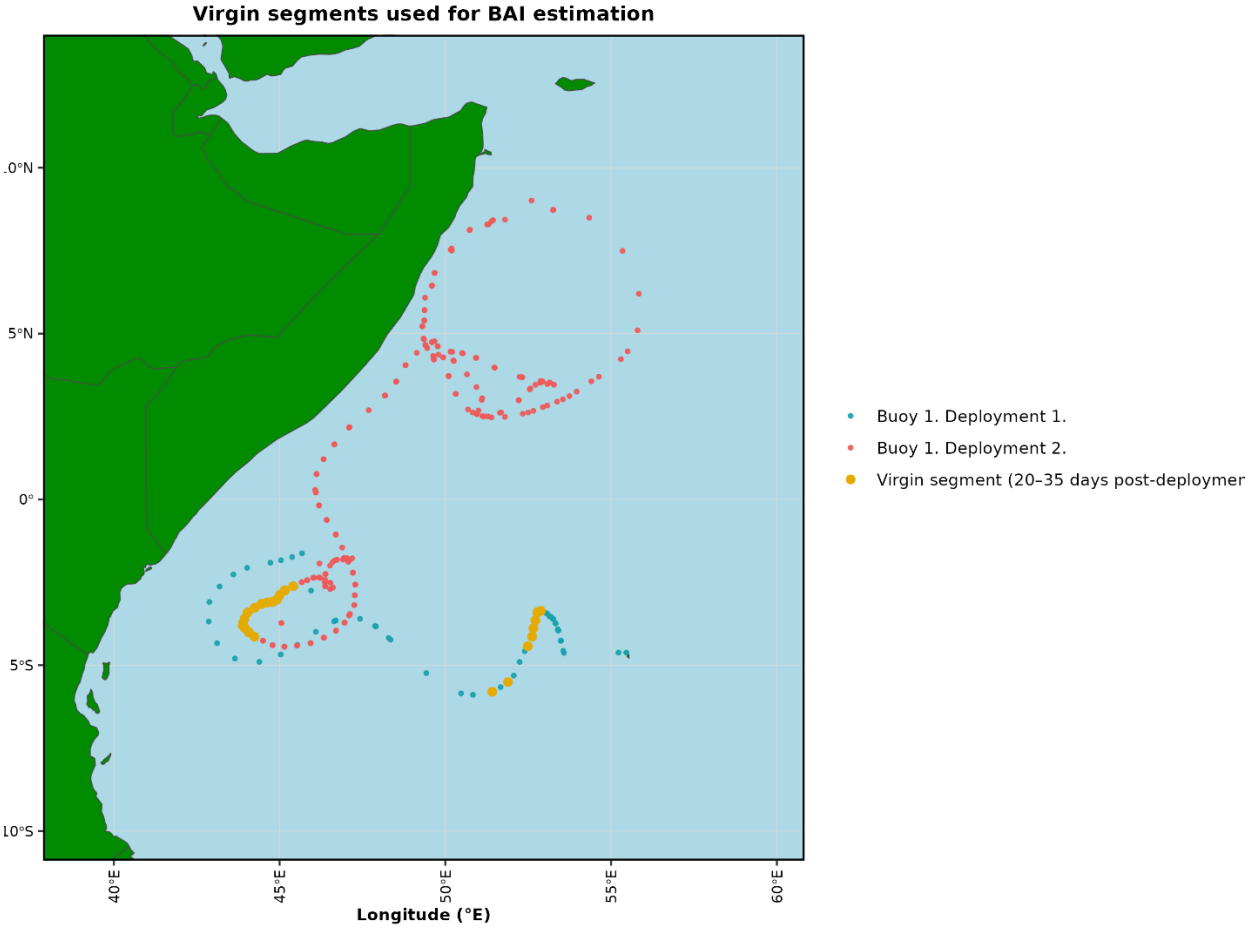

Figure 2. Example of "virgin" segments used for the calculation of the BAI index. Trajectories correspond to a single buoy with two different paths representing drifts of different FADs. A virgin segment is defined as the segment of a buoy trajectory whose associated FAD likely represents a new deployment, which has been potentially colonized by tuna and not already fished. We consider as virgin segments (i.e. when tuna has aggregated to FAD) those segments of trajectories from 20-35 days at sea. "Virgin" segments are shown gold coloured.

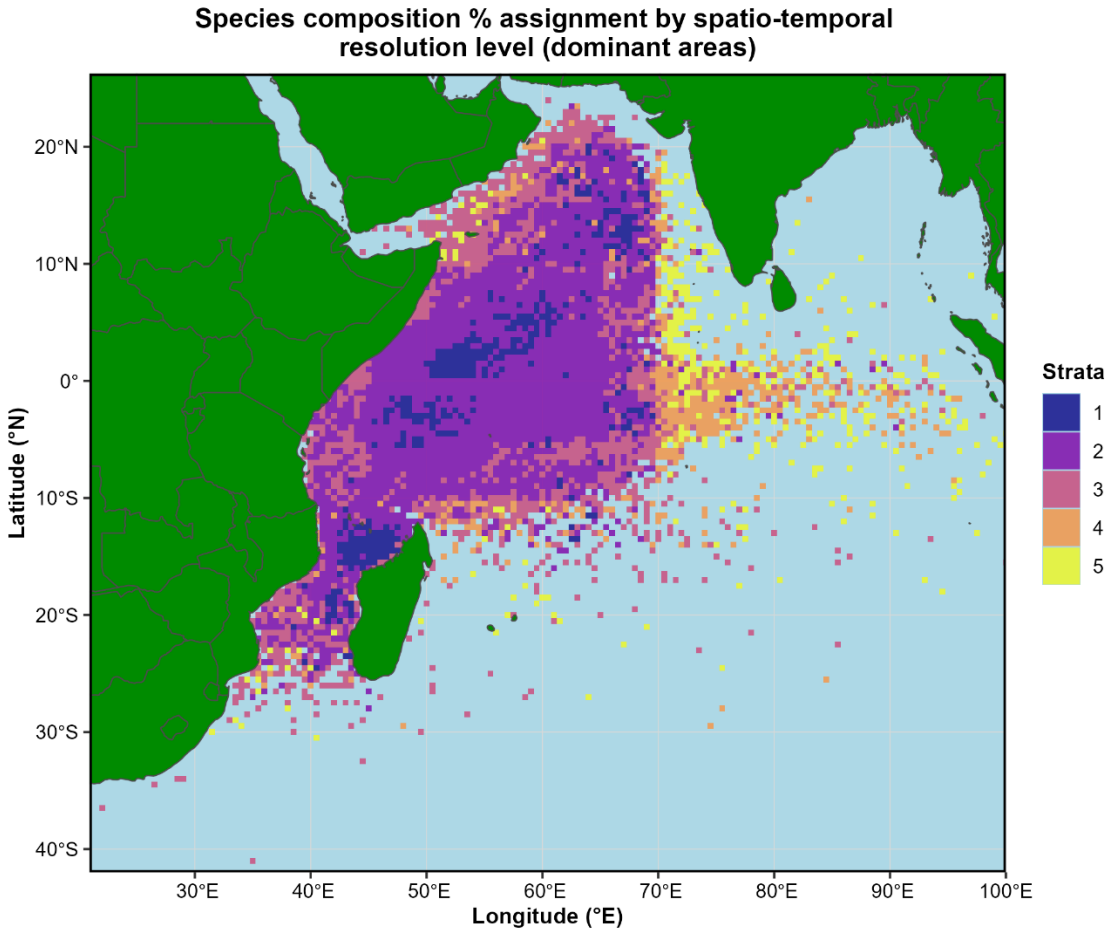

Figure 3. Spatial distribution of species composition percentage assignment by spatio-temporal resolution level across a 5 x 5º grid for the period 2012–2024. Colored cells represent the dominant stratum category (1 to 5) determined by the highest frequency of observations within each cell.

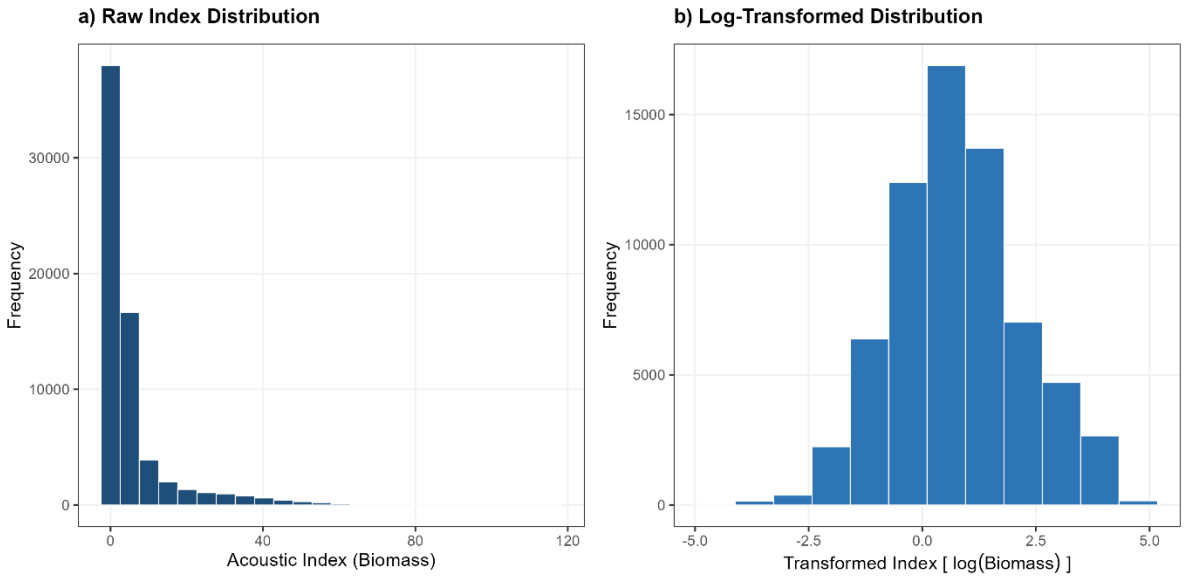

Figure 4. Histograms of the nominal values (left) and the log transformed nominal values (right) of the Buoy-derived Abundance Index (0.9 quantile of the integrated acoustic energy observations in "virgin" sequences).

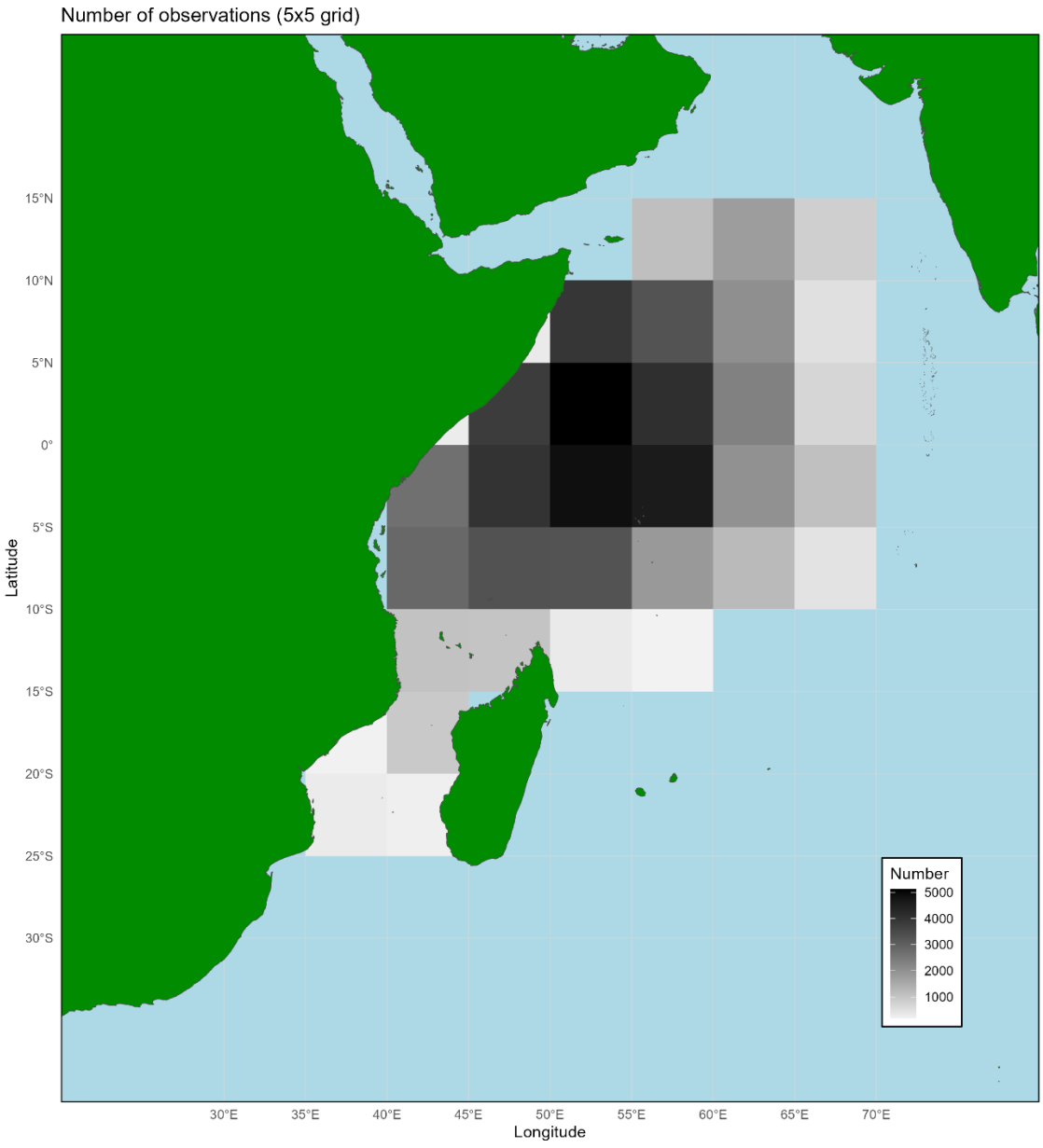

Figure 5. Spatial distribution [5ºx5º] of the "virgin" sequences of buoy trajectories that have been used in the GLM analysis.

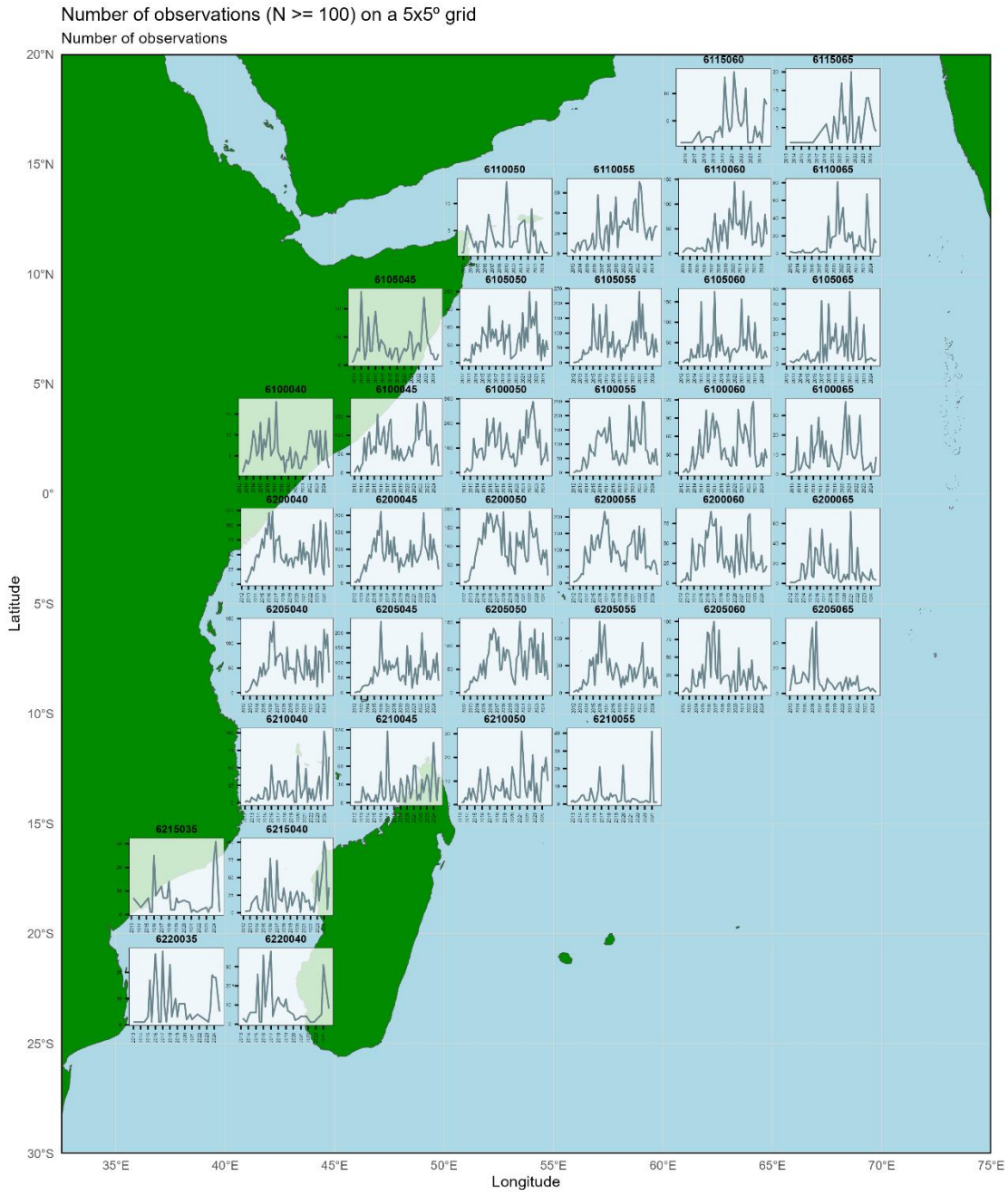

Figure 6. Quarterly evolution of the number of observations ("virgin" sequences of buoy trajectories) on a 5ºx5º grid.

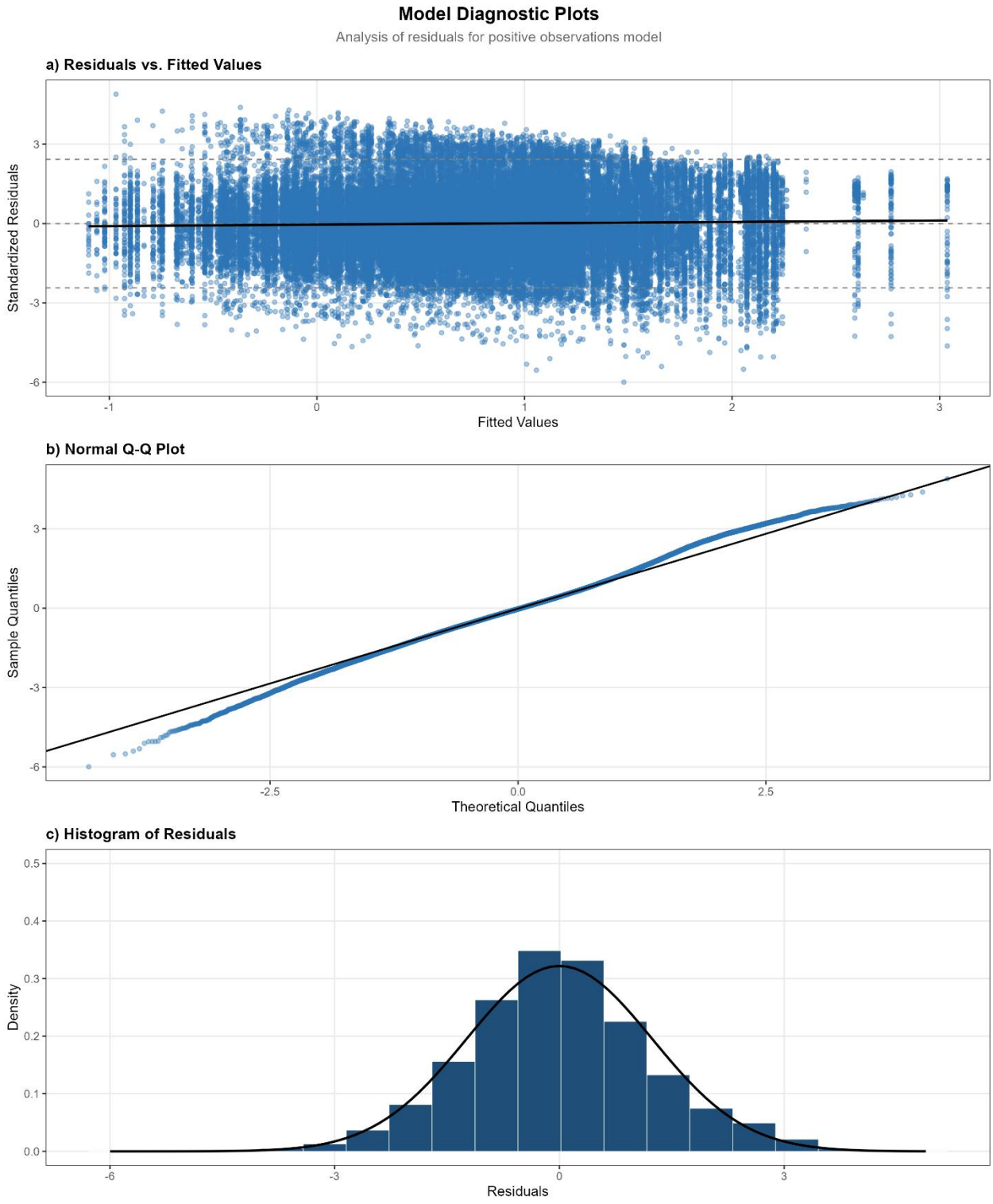

Figure 7. Diagnostics of the lognormal model selected for the period 2012-2024: residuals vs fitted, Normal Q-Q plot and frequency distributions of the residuals.

a)

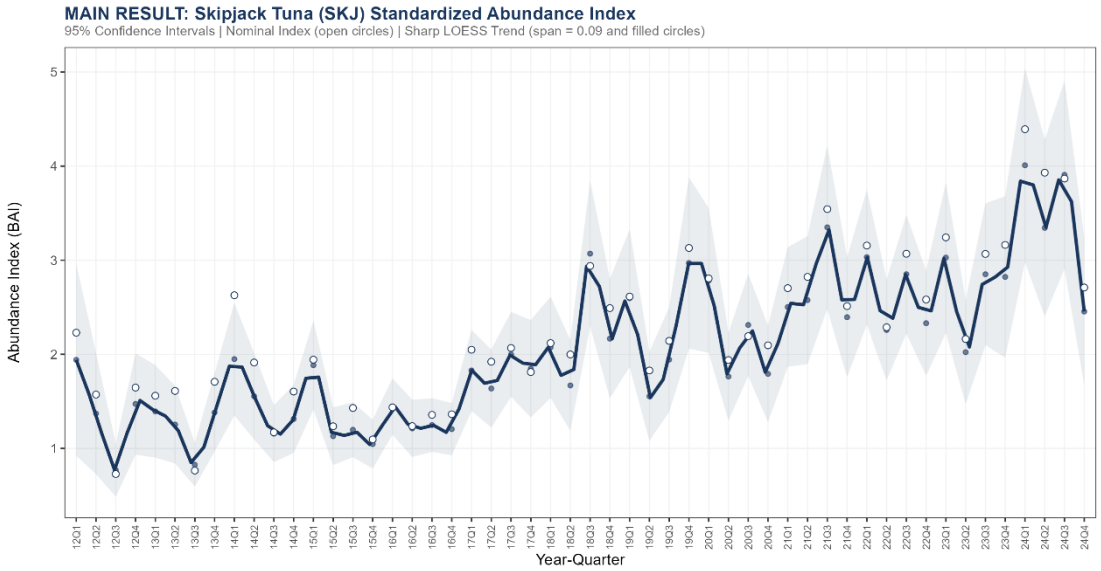

b)

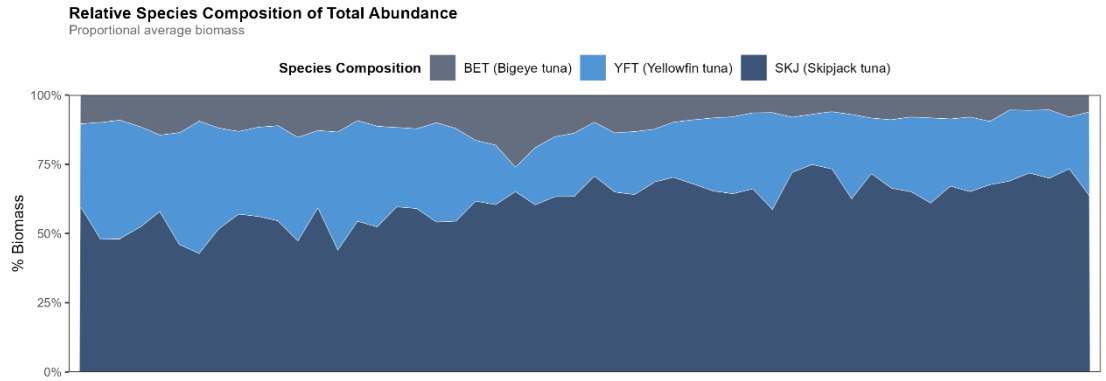

c)

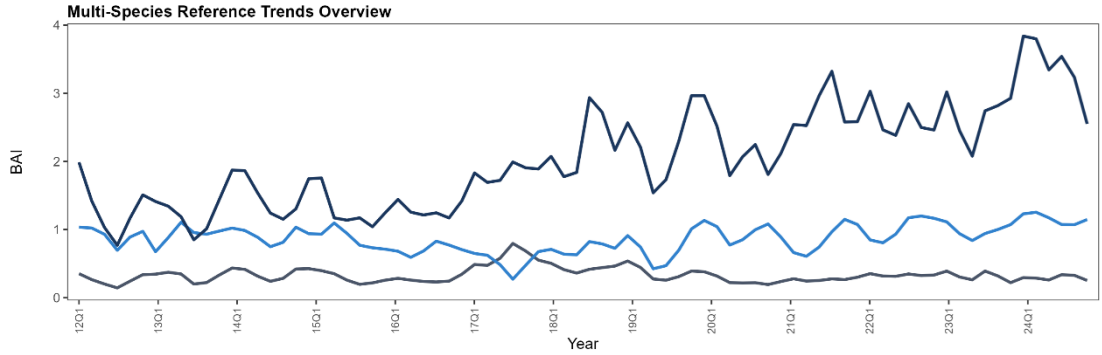

Figure 8. Time series of nominal (circles) and standardized (continuous line) Buoy-derived Abundance Index for the period 2012–2024. (a) Main standardized trend for Skipjack tuna (SKJ) with its 95% upper and lower confidence intervals (shaded ribbon); (b) Relative species composition (%) per quarter stacked from lowest (BET) to highest (SKJ) proportion; and (c) Comparative historical trajectories for the three tropical tuna species (SKJ, YFT, and BET).

REFERENCES

Amante, C., & Eakins, B. (2009). ETOPO1 1 arc-minute global relief model: procedures, data sources and analysis. NOAA Technical Memorandum NESDIS NGDC-24. *National Geophysical Data Center, NOAA*, *10*, V5C8276M.

Baidai, Y. D. A. (2020). *Derivation of a direct abundance index for tropical tunas based on their associative behavior with floating objects* Université Montpellier].

Bates, D., Mächler, M., Bolker, B., & Walker, S. (2014). Fitting linear mixed-effects models using lme4. *arXiv preprint arXiv:1406.5823*.

Boyra, G., Moreno, G., Orue, B., Sobradillo, B., & Sancristobal, I. (2019). In situ target strength of bigeye tuna (Thunnus obesus) associated with fish aggregating devices. *ICES Journal of Marine Science*, *76*(7), 2446-2458.

Boyra, G., Moreno, G., Sobradillo, B., Pérez-Arjona, I., Sancristobal, I., & Demer, D. A. (2018). Target strength of skipjack tuna (Katsuwanus pelamis) associated with fish aggregating devices (FADs). *ICES Journal of Marine Science*, *75*(5), 1790-1802.

Capello, M., Deneubourg, J. L., Robert, M., Holland, K. N., Schaefer, K. M., & Dagorn, L. (2016). Population assessment of tropical tuna based on their associative behavior around floating objects. *Scientific Reports*, *6*(1), 36415. https://doi.org/10.1038/srep36415

Foote, K. G. (1983). Linearity of fisheries acoustics, with addition theorems. *The Journal of the Acoustical Society of America*, *73*(6), 1932-1940.

Gaertner, D., Ariz, J., Bez, N., Clermidy, S., Moreno, G., Murua, H., & Soto, M. (2016). Objectives and first results of the CECOFAD project. *Collective Volume of Scientific Papers*, *72*(2), 391-405.

Gaertner, D., Clermidy, S., Ariz, J., Bez, N., Moreno, G., Murua, H., Soto, M., & Marsac, F. (2016). Results achieved within the framework of the EU research project: Catch, Effort, and eCOsystem impacts of FAD-fishing (CECOFAD). *Acta Agriculturae Slovenica*.

Hampton, I. (1996). Acoustic and egg-production estimates of South African anchovy biomass over a decade: comparisons, accuracy, and utility. *ICES Journal of Marine Science*, *53*(2), 493-500.

Katara, I., Gaertner, D., Marsac, F., Grande, M., Kaplan, D., Urtizberea, A., Abascal, F. . (2018). *Standardisation of yellowfin tuna CPUE for the EU purse seine fleet operating in the Indian Ocean. 20th session of the Working Party on Tropical Tuna.*

Lo, N. C.-h., Jacobson, L. D., & Squire, J. L. (1992). Indices of relative abundance from fish spotter data based on delta-lognornial models. *Canadian journal of fisheries and aquatic sciences*, *49*(12), 2515-2526.

Lopez, J., Moreno, G., Sancristobal, I., & Murua, J. (2014). Evolution and current state of the technology of echo-sounder buoys used by Spanish tropical tuna purse seiners in the Atlantic, Indian and Pacific Oceans. *Fisheries Research*, *155*, 127-137.

Masse, J., Uriarte, A., Angélico, M., & Carrera, P. (2018). Pelagic survey series for sardine and anchovy in ICES subareas 8 and 9—Towards an ecosystem approach. *ICES cooperative research report*(332).

Maunder, M. N., & Punt, A. E. (2004). Standardizing catch and effort data: a review of recent approaches. *Fisheries Research*, *70*(2), 141-159.

Maunder, M. N., Sibert, J. R., Fonteneau, A., Hampton, J., Kleiber, P., & Harley, S. J. (2006). Interpreting catch per unit effort data to assess the status of individual stocks and communities. *ICES Journal of Marine Science: Journal du Conseil*, *63*(8), 1373-1385.

Moreno, G., Dagorn, L., Capello, M., Lopez, J., Filmalter, J., Forget, F., Sancristobal, I., . and Holland, K. . (2016). Fish aggregating devices (FADs) as scientific platforms. *Fisheries Research*, *178: 122-129*. https://doi.org/http://dx.doi.org/10.1016/j.fishres.2015.09.021

Orue, B., Lopez, J., Moreno, G., Santiago, J., Boyra, G., Uranga, J., & Murua, H. (2019). From fisheries to scientific data: A protocol to process information from fishers' echo-sounder buoys. *Fisheries Research*, *215*, 38-43.

Quinn, T. J., & Deriso, R. B. (1999). *Quantitative fish dynamics*. oxford university Press.

Røttingen, I. (1976). On the relation between echo intensity and fish density.

Santiago, J., Lopez, J., Moreno, G., Murua, H., Quincoces, I., & Soto, M. (2016). Towards a tropical tuna buoy-derived abundance index (TT-BAI). *Collect. Vol. Sci. Pap. ICCAT*, *72*(3), 714-724.

Santiago, J., Uranga, J., Quincoces, I., Grande, M., Murua, H., Merino, G., Zudaire, I., Urtizberea, A., & Boyra, G. (2021a). INDEX OF ABUNDANCE OF JUVENILE BIGEYE TUNA IN THE ATLANTIC OCEAN DERIVED FROM ECHOSOUNDER BUOYS (2010-2020). *Collect. Vol. Sci. Pap. ICCAT*, *78*(2), 231-252.

Santiago, J., Uranga, J., Quincoces, I., Grande, M., Murua, H., Merino, G., Zudaire, I., Urtizberea, A., & Boyra, G. (2021b). INDEX OF ABUNDANCE OF SKIPJACK TUNA IN THE ATLANTIC OCEAN DERIVED FROM ECHOSOUNDER BUOYS (2010-2020). *Collect. Vol. Sci. Pap. ICCAT*, *79*(1), 158-175.

Santiago, J., Uranga, J., Quincoces, I., Orue, B., Grande, M., Murua, H., Merino, G., Urtizberea, A., Pascual, P., & Boyra, G. (2019). *A Novel Index of Abundance of Juvenile Yellowfin Tuna in the Indian Ocean Derived from Echosounder Buoys*.

Santiago, J., Uranga, J., Quincoces, I., Orue, B., Grande, M., Murua, H., Merino, G., Urtizberea, A., Pascual, P., & Boyra, G. (2020). A novel index of abundance of juvenile yellowfin tuna in the Atlantic Ocean derived from echosounder buoys. *Collect. Vol. Sci. Pap. ICCAT*, *76*(6), 321-343.

Scott, G. P., & Lopez, J. (2014). *The use of FADs in Tuna Fisheries. European Parliament. Policy Department B: Structural and Cohesion Policies: Fisheries*.

Simmons, E., & MacLennan, D. (2005). Fisheries acoustics. *Theory and Practice. Second edition published by Blackwell Science*.

Sobradillo, B., Boyra, G., Uranga, J., & Moreno, G. (2024). Target strength measurements of yellowfin tuna (Thunnus albacares) and acoustic discrimination of three tropical tuna species. *ICES Journal of Marine Science*, *81*(5), 850-863.

Torres-Irineo, E., Gaertner, D., Chassot, E., & Dreyfus-León, M. (2014). Changes in fishing power and fishing strategies driven by new technologies: The case of tropical tuna purse seiners in the eastern Atlantic Ocean. *Fisheries Research*, *155*, 10-19.

Uranga, J. L., J. Grande, M. Lennert-Cody, C. Quincoces, I. Granado, I. Maunder, M. Aires-da-Silva, A. Merino, G. Murua, H., Santiago, J. (2021). *Tropical tuna biomass indicators from echosounder buoys in the eastern pacific ocean.*

Uranga, J. L., J. Grande, M. Lennert-Cody, C. Quincoces, I. Granado, I. Maunder, M. Aires-da-Silva, A. Merino, G. Murua, H., Santiago, J. (2023). *UPDATED TROPICAL TUNA BIOMASS INDICES FROM ECHOSOUNDER BUOYS IN THE EASTERN PACIFIC OCEAN*.

Uranga, J. L., J. Grande, M. Lennert-Cody, C. Quincoces, I. Granado, I. Maunder, M. Aires-da-Silva, A. Merino, G. Murua, H., Santiago, J. (2024). *ECHOSOUNDER BUOY DERIVED TROPICAL TUNA BIOMASS INDICES IN THE EASTERN PACIFIC OCEAN*

Wain, G., Guéry, L., Kaplan, D. M., & Gaertner, D. . (2021). Quantifying the increase in fishing efficiency due to the use of drifting FADs equipped with echosounders in tropical tuna purse seine fisheries. *ICES Journal of Marine Science*, *78(1), 235-245.*

Wessel, P., and W. H. F. Smith (1996). A global, self-consistent, hierarchical, high-resolution shoreline database. *J. Geophys. Res*, *101(B4), 8741-8743*. https://doi.org/10.1029/96JB00104